Suplemento de la Revista Mexicana de Física **3** 0308026 (2022) 1–6

Hyperon physics at HADES as a fair phase-0 experiment

G. Perez-Andrade[a], R. Lalik[b], J. Ritman[c,a], P. Salabura[b] and P. Wintz[a] for the HADES and PANDA Collaborations
[a] *Forschungszentrum Juelich GmbH, 52428 Juelich, Germany.*
[b] *Smoluchowski Institute of Physics, Jagiellonian University of Cracow, 30-059 Krakaw, Poland.*
[c] *GSI Helmholtzzentrum für Schwerionenforschung GmbH, Darmstadt, Germany.*
Ruhr-University Bochum, Universitätsstraße 150 44801 Bochum.

Received 14 January 2022; accepted 2 March 2022

The HADES experiment investigates the nuclear matter and the properties of baryonic resonances. As part of the FAIR Phase-0 program, HADES is being upgraded to enable a wide range of experiments, including investigating electromagnetic decays of hyperons produced in proton-induced reactions. Feasibility studies show that the newly installed forward detectors are crucial for hyperon reconstruction. The detector upgrade and feasibility studies in preparation for the upcoming beamtimes are presented.

Keywords: FAIR phase-0; hyperon electromagnetic decays; straw tube (tracker).

DOI: https://doi.org/10.31349/SuplRevMexFis.3.0308026

1. Introduction

The High Acceptance Di-Electron Spectrometer (HADES) is a fixed-target experiment where ion and proton-induced reactions are used to study strangeness production, the emissivity of resonance matter, and the electromagnetic structure of baryonic resonances [1–3]. HADES is in operation at the Heavy-ion Synchrotron (SIS18) accelerator, at the GSI Helmholtz Center for Heavy Ion Research in Darmstadt, Germany, and is also part of the new Facility for Antiprotons and Ions Research (FAIR), under construction at GSI. The FAIR Phase-0 program includes single, multi-strange hyperon production and the study of hyperon electromagnetic decays. The HADES collaboration already performed studies of p+p and p+Nb collisions at T = 3.5 GeV [4]. However, higher statistics are needed for a better understanding of the hyperon production and decay mechanism.

Baryon structure can be explored through the study of its electromagnetic decays. These provide access to electromagnetic Transition Form Factors (eTFFs), which are functions of the momentum transfer squared (q^2) of the virtual photon exchanged in the process. The eTFFs can be studied in different kinematic regions: space-like ($q^2 < 0$) in electron scattering experiments, and time-like ($q^2 > 0$) via e^+e^- annihilation and Dalitz decays of baryonic resonances (*e.g.* $Y^* \rightarrow \Lambda e^+e^-$). The $q^2 = 0$ case corresponds to radiative decays (*e.g.* $Y^* \rightarrow \Lambda\gamma$). HADES results on Dalitz decays in the non-strange sector agree well with the Vector Meson Dominance (VMD) model [8]. In this model, an important contribution to the transition is attributed to an intermediate ρ vector meson which could be explained as pion cloud effects, as suggested by calculations performed within the spectator quark model [7–9]. Pion cloud effects have also been proposed to explain the larger than expected observed decay width in the $\Sigma(1385)^0 \rightarrow \Lambda\gamma$ transition [10]. Several theoretical models such as the NRQM [11–14], the Relativized Constituent Quark Model (RCQM) [15], and the MIT bag model [16] have been proposed to explain the hyperon wave functions. However, more experimental input is needed to find a model that provides a complete data description. First measurements of the elastic magnetic form factors of hyperons such as Λ and $\Sigma^{\pm}$, produced at a momentum transfer $q^2 = 14$ GeV^2 in e^+e^- annihilation were already provided by the CLEO collaboration [17]. However, to this date, there are no measurements of hyperon Dalitz decays, which will shed light on hyperon structure at lower q^2 values, where mesonic degrees of freedom are expected to dominate. In addition, such measurements will establish a link to existing measurements in the space-like region.

Another topic of the FAIR phase-0 program is the production of double-strange hyperons. So far, very little is known about multi-strange hyperons produced at low q^2. Observations made in previous HADES studies show that the Ξ^- production yield in Ar+KCl at 1.75 GeV [18], and in p+Nb at 3.5 GeV [4] collisions, is higher than expected according to model calculations [19]. This puzzling result calls for new measurements.

In general, future HADES data from p+p collisions will provide important references of expected strangeness enhancements in heavy-ion collisions. The double-strangeness topic also covers studies about the poorly known hyperon-hyperon interaction. The Λ-Λ interaction plays an essential role in neutron star core studies and the Ξ production mechanism [20]. These will be complementary measurements to those planned at PANDA, in which the Λ-Λ and $\bar{\Lambda}$-Λ production will be studied in $p + p$ and $\bar{p} + p$ collisions, respectively [21].

1.1. HADES spectrometer upgrade

HADES has been in operation at the SIS18 since 2002 to study proton, pion, and heavy-ion induced reactions with beam energies in the GeV range, incident on a fixed target (proton or nuclear). HADES is characterized by its large azimuthal acceptance (85%) over a polar angle range between $\theta = 18°$ and 85°, achieved with six identical detector systems delimited by superconducting coils that produce a toroidal magnetic field [5, 6].

At FAIR, proton beams with energies up to 29 GeV will be available, opening the possibility to study many interesting processes and imposing specific experimental requirements. For HADES, an upgrade of the existing detector and data-acquisition systems, and the installation of new components are thus required. For example, changes to the RICH system have improved the dilepton identification [22], and gamma reconstruction is now possible thanks to a new Electromagnetic Calorimeter [23]. Furthermore, the faster HADES DAQ system will allow for operation with up to 200 kHz average trigger rate. Some of the latest additions to HADES consists of new detectors as part of a Forward Detector: the Straw Tracking Stations (STS) and a Forward Resistive Plate Chamber (fRPC) for time-of-flight measurements. The STS system is part of the FAIR Phase-0 which allows an early operation of these straw systems under experiment conditions. The STS will become part of the Forward Tracker (FT) in PANDA at the start of the FAIR phase-1. It is foreseen that the increased count rates expected with the upgraded system will enable the successful reconstruction of all the channels included in the hyperon program.

2. The Forward detector system (FD)

The new FD system extends the polar angle acceptance of the HADES spectrometer to the region between θ = 0.75 and 7°. As explained below, it was found that most pions originating from Λ decay are within the HADES acceptance. In contrast, a high fraction of the decay protons is detected in the FD, highlighting its importance for hyperon reconstruction [24].

2.1. Straw tracking stations (STS)

The Straw Tracking Stations STS1 and STS2 have four double layers of gas-filled straws each (Fig. 1). The straws design is the same for both stations and is based on the Straw Tube Tracker (STT) [25] and Forward Tracker (FT) of the PANDA experiment [26, 27]. Each straw is made of 27μm thin Al-Mylar walls and has a 20 μm thin gold-plated W/Re wire extending along its axis. The straws inner diameter is 10 mm, and their length is 76 cm and 125 cm for STS1 and

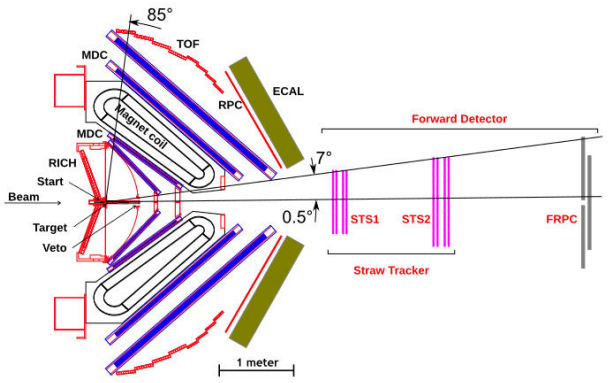

FIGURE 1. Schematic cross-sectional view of the HADES spectrometer. The STS and fRPC detectors are shown in magenta and gray, respectively. Figure from [24].

and STS2, respectively. The gas mixture used is Ar/CO_2 (90:10) operated at 1 bar over-pressure. The latter makes the straws self-supporting, reducing the need for a support structure. Four azimuthal orientations of the STS are chosen to resolve ambiguities in multi-track events. The orientation of the first and last double layers of STS1 is $\phi = 90°$, whereas the second and third double layers are aligned at ϕ = 0°. On the other hand, the azimuthal orientation of the double layers in STS2 are ϕ = 0°, 90°, 45°, -45°. The straw charge signals are amplified and shaped by the PASTTREC-ASICs on front-end mounted electronic boards [25, 28]. The leading edge time t_{LE} and trailing edge time t_{TE} are measured in multi-hit TDCs implemented in the Trigger Readout Board version 3 (TRB3) [26]. From pre-commissioning tests a spatial resolution of 0.13 mm (σ) was determined for MIPs[i] [27].

2.2. Forward restive plate chambers (FRPC)

The FRPC is designed for time of flight measurements, and it is located at about 7.5 m downstream from the target (Fig. 1). The FRPC design has four sectors. Each is composed of two layers of 16 individually shielded hybrid (metal glass) strip-like RPCs [29]. The layers within one sector are partially overlapped. The length of the counters is 750 mm, and to account for particle flux variations, two different widths are used: 22 mm and 42 mm [24, 30]. High voltage is applied to the central aluminum electrode where the signals are collected, and the time of flight and Time over Threshold are measured using the TRB3. The fRPC should be able to measure particle rates of 320 Hz/cm^2 with an efficiency of at least 90%. Preliminary tests show an efficiency of $>$ 85 - 90 %, and a time resolution of $<$ 100 - 120 ps.

2.3. Track reconstruction in the FD

The track reconstruction for these simulation feasibility studies was performed in two stages and is described in detail at [24]. In the first or low-resolution (LR) stage, only the straws wire coordinates are taken into account, providing a spatial resolution limited to the straw pitch/$\sqrt{12}$. The track candidate is then matched with a hit in the fRPC. In the second stage, also called high-resolution (HR), the hits within each double layer are clustered and fitted with straight lines. A track fitting procedure is then performed. Two algorithms were tested: one based on the CBM-MUCH [31], which uses the Least Squares Method (LSM), and one based on the COSY-TOF detector [32], which is based on χ^2 minimization using Minuit. It was concluded that the χ^2 method gives a better solution [24]. Track candidates are then rejected based on its χ^2 value, assuming a tracking resolution of σ = 200 μm. The accepted track candidates are sorted, and if two tracks within one event share at least half of the straws, the one with the smallest χ^2 is kept. Since the FD is located in a magnetic field-free area, a direct momentum reconstruction is not possible. However, this is done by selecting a mass hypothesis *e.g.* proton and combining its track path length information with the measured time of flight measured in the fRPC.

TABLE I. Expected count rates of studied channels. Results extracted from [24].

Process	σ [μb]	BR	acc $\times\epsilon$[%]	Counts/day (LH_2)
$\Sigma(1385)^0 \to \Lambda\gamma$	56	9.07 $\times 10^{-3}$	0.030	99
$\Lambda(1520) \to \Lambda\gamma$	69	7.03 $\times 10^{-3}$	0.026	82
$\Sigma(1385)^0 \to e^+e^-$	56	8.94 $\times 10^{-5}$	0.48	15
$\Lambda(1520) \to e^+e^-$	69	6.93 $\times 10^{-5}$	0.58	18
$\Xi^- \to p\pi^-\pi^-$	3.6	0.64	1.68	2.43 $\times 10^4$
$\Xi^- \to p\pi^-\pi^-$	0.35	0.64	1.68	2.43 $\times 10^3$
$pp \to \Lambda\Lambda K^+K^+$	3.6	0.64^2	0.34	3.15 $\times 10^3$
$pp \to \Lambda\Lambda K^+K^+$	0.35	0.64^2	0.34	3.15 $\times 10^2$

3. Simulation feasibility studies

Detailed simulation studies were done to test the performance of the upgraded HADES in measuring different benchmark channels of the hyperon program. The simulations were generated with the Pluto Monte-Carlo event generator [33], the detector acceptance modeled with GEANT3, and the reconstructions executed using the HADES software framework called Hydra [34]. All simulations were performed for a proton beam with T = 4.5 GeV impinging upon a 4.7 cm long LH_2 target. The reconstruction strategies were also tested in the dominant background channels for each case. Since there is little information on production cross-sections (σ) of most of the analyzed channels at 4.5 GeV, these were extrapolated or calculated from measurements at other energies. Moreover, all (except radiative decays) assume a semi-inclusive reconstruction tagged by a Λ reconstruction. The complete list of background channels and further details of these simulation studies can be found at [24]. Here only the main steps of the analysis and results are summarized.

3.1. Hyperons reconstruction

A common aspect of all studied channels is the reconstruction of protons and pions originating from Λ hyperon decays. The kinematics of hyperon decays in fixed-target experiments results in the daughter baryons showing a strong forward boost in the laboratory frame. The small decay phase space and mass difference between the daughters of Λ decay lead to the proton being emitted in a direction close to the Λ hyperon, and the pions being emitted in a wider angular range [35]. Most pions stay within the HADES acceptance, whereas the protons preferably reach the FD. This is similar for Ξ^- decay products. The latter is taken into account for the particle identification process since, in most cases, it is assumed that particles detected within the FD acceptance are protons. In contrast, the particles detected within the HADES acceptance are pions. Overall it was found that in 41% of the cases, protons from $\Lambda(1520)$ decays are detected within the FD acceptance, 88% of the Ξ^- events have both pions reconstructed within HADES and the proton within the FD. Finally, 89% of the $\Lambda\Lambda$ events include at least one particle within the FD [24].

3.2. Hyperon electromagnetic decays

The investigated reactions are of the type $p + p \to pK^+Y^*$, where Y^* can be $\Sigma(1385)^0$, $\Lambda(1405)$ or $\Lambda(1520)$. The production cross section calculations were based on COSY, COSY-TOF, HADES and ANKE data [36–41]. Both radiative ($Y^* \to \Lambda\gamma$) and Dalitz decays ($Y^* \to \Lambda e^+e^-$) were studied for each Y^*. Branching ratios (BR) obtained by the CLAS Collaboration were used for the radiative decays [10, 42], and also to estimate the BR of Dalitz decays. Cross section and BR values are shown in Table I.

The study of radiative decays required exclusive reconstruction to suppress high background contributions originating from neutral pion decays. An Artificial Neural Network (ANN) implemented with the PyTorch framework [43] was used for final state hadron identification, and ECAL clusters in correlation with RPC hits are used to identify photon candidates. The Λ candidates are formed by combining all proton and pions candidates, and specific topological cuts are used to select the signal events better. The resulting invariant mass distribution M($\Lambda\gamma$) of signal together with the background can be seen in Fig. 2a). Two prominent signal peaks can be seen in the $\Sigma(1385)$ and $\Lambda(1520)$ mass regions. The slight shift in the distribution is attributed to the ECAL response function.

For Dalitz decays, inclusive reconstruction was performed. Specific ranges of the measured momentum and β were selected to identify pions and protons, whereas the e^+e^- are identified by matching reconstructed tracks to hits in the RICH detector [44]. A pion and a proton candidates are then combined into the mother Λ candidates, and cuts based on the topology of the reaction are applied to reject background. In this case, the primary background contributions come from channels with a Λ and a di-lepton source in the final state. The final invariant mass distribution M(Λe^+e^-) is shown in Fig. 2b). The corresponding mass peaks of the $\Sigma(1385)^0$ and $\Lambda(1520)$ resonances can be clearly seen on top of the Δ Dalitz decay background.

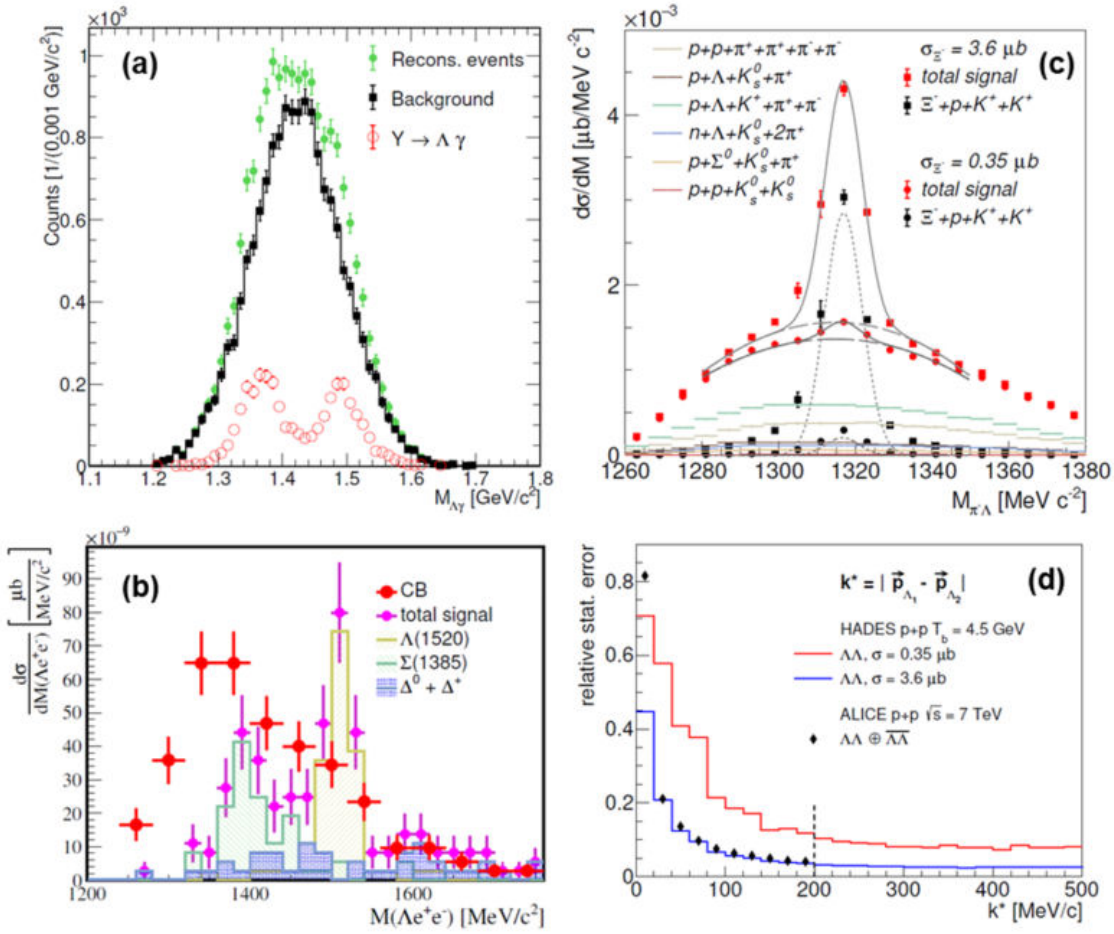

FIGURE 2. a) Reconstructed invariant mass distribution of $\Lambda\gamma$. The background channels have $pK^+\Lambda$ in the final state, or correspond to multipion channels. b) Reconstructed invariant mass distribution of Λe^+e^-. The most prominent background comes from π^0 and Δ Dalitz decays. c) Reconstructed invariant mass distribution of $\Lambda\pi$ for both BR estimations (red symbols). True (background subtracted) events are also shown (black symbols). d) Relative statistical error of $\Lambda\Lambda$ yield for both cross section assumptions.

The calculated BR for the $\Lambda(1405)$ was two orders of magnitude smaller than that of the $\Sigma(1385)^0$ and $\Lambda(1520)$ in both radiative and Dalitz decays. In consequence, the resulting yield is too small to be measured. However, the $\Lambda(1405)$ hadronic decay has already been measured by HADES [45].

3.3. Production of double strangeness

The production of double strangeness is studied in the reaction $p + p \rightarrow pK^+K^+\Xi^-$. Two estimates of the Ξ^- production cross-section were used: an upper limit obtained from HADES data from p+Nb interactions [4], and a lower limit extrapolated from p+p collisions at higher energies. The values are shown in Table I. The particle identification was based on selection bands generated with the β vs. momentum correlation for specific mass and momentum hypotheses. The Ξ^- reconstruction is performed in two steps. First, a Λ candidate is reconstructed by combining proton candidates identified within HADES or the FD with pion candidates identified in HADES. Then, the Λ candidates are combined with pion candidates detected within the HADES acceptance only. The highest background contribution, in this case, is generated from channels with multi-pion production. However, this is successfully suppressed by imposing a constraint on the location of the Λ candidates displaced vertex. Additional topological cuts are also applied to reduce the background further. The final M($\Lambda\pi^-$) reconstructed invariant mass is shown in Fig. 2c) for both cross-section estimates. This figure also shows the Ξ^- true signal events and the main background channels. The signal is clearly visible above the background for the upper limit of cross-section, whereas the lower limit case is less prominent although still measurable.

To address the topic of hyperon-hyperon interactions, the $p + p \rightarrow \Lambda\Lambda K^+K^+$ reaction was studied. The same exclusive cross-sections as the one used for the cascade channel were used, given their similarities in *e.g.* meson number, strange quark content and phase space. The particle identification and Λ reconstruction was performed in a similar way as in the previous cases, with changes depending on this reaction's topology. For instance, in this case, both Λ particles

are generated at the primary vertex, as opposed to the Ξ^- decay. By studying this channel, the correlations between the two reconstructed Λs can be examined. Figure 2d) shows the statistical precision for the relative momentum spectrum (k^*) for events reconstructed in this study, together with results published by ALICE. It can be concluded that with the upper σ estimate, results similar to those obtained by ALICE can be achieved. Moreover, in the lower k^* region HADES is expected to improve the precision.

3.4. Results

The count rates for all the analyzed channels were calculated and are shown in Table I. The estimations shown here take into account the acceptance times reconstruction efficiency in each case, a beam duty cycle of 50% and a luminosity of $\mathcal{L} = 1.5 \times 10^{31}$ cm^{-2}s^{-1} for the LH_2 target.

4. HADES commissioning beamtime

The installation of the full STS system and two out of four fRPC sectors in HADES was completed at the end of 2020. These components have also been included in the HADES DAQ. In February 2021, a dedicated commissioning beamtime was carried out to test the newly added forward detector system and the upgraded DAQ system under experiment conditions. The SIS18 delivered proton beams with T = 2 and 4.2 GeV kinetic energy with particle rates of up to 10^8 p/s, onto the LH_2 target. The STS and fRPC showed stable operation, without failures. The collected data is being used to develop calibration methods, data-taking, and software for the analysis.

5. Conclusions and outlook

Studies of hyperon production and decays are important aspects of the FAIR Phase-0 program. The HADES spectrometer has undergone a major hardware upgrade to face the challenges that come with its operation at FAIR. Feasibility simulation studies have shown that with these upgrades, HADES is well prepared for the planned physics program. A four weeks production beamtime with the upgraded HADES is scheduled for February 2022 [46].

---

i. MIPs stands for Minimum Ionizing Particles.

1. J. Adamczewski-Musch *et al.* [HADES], Sub-threshold production of K_s^0 mesons and Λ hyperons in Au+Au collisions at $\sqrt{s_{NN}}$ = 2.4 GeV, Phys. Lett. B **793** (2019), 457-463
2. J. Adamczewski-Musch *et al.* [HADES], Probing dense baryon-rich matter with virtual photons, Nature Phys. **15** (2019) no.10, 1040-1045
3. J. Adamczewski-Musch *et al.* [HADES], Analysis of the exclusive final state npe$^+$e$^-$ in quasi-free np reaction, Eur. Phys. J. A **53** (2017) no.7, 149
4. G. Agakishiev *et al.*, Subthreshold Ξ^- Production in Collisions of p (3.5 GeV)+Nb ,Phys. Rev. Lett. **114**, 212301 (2015).
5. G. Agakishiev *et al.* [HADES], The High-Acceptance Dielectron Spectrometer HADES, Eur. Phys. J. A **41** (2009), 243-277
6. R. Schicker, *et al.*, Acceptance and resolution simulation studies for the dielectron spectrometer HADES at GSI, Nucl. Instrum. Meth. A **380**, 586-596 (1996)
7. J. Adamczewski-Musch *et al.*, $\Delta(1232)$ Dalitz decay in proton-proton collisions at T=1.25 GeV measured with HADES at GSI, Phys. Rev. C **95**, 065205 (2017).
8. G. Ramalho and M.T. Pena, Timelike $\gamma^* N \to \Delta$ form factors and Δ Dalitz decay , Phys. Rev. D **85**, 113014 (2012).
9. G. Ramalho, Low-Q^2 empirical parametrizations of the N^* helicity amplitudes ,Phys. Rev. D **100**, 114014 (2019).
10. D. Keller *et al.*, Branching ratio of the electromagnetic decay of the $\Sigma^+(1385)$, Phys. Rev. D **85**, 052004 (2012).
11. N. Isgur and G. Karl. P Wave Baryons in the Quark Model, Phys. Rev. D **18** (1978), p. 4187. **18**.4187.
12. M.Horbatsch *et. al.*, Photon decays of baryons with strangeness, Phys. Rev. D **28**.1125 (1983).
13. R.Koniuk and N.Isgur. Photon decays in quark model with chromodynamics, Phys. Rev. D **21**.1868 (1981).
14. E.J.Moniz *et. al.*, Hyperon radiative decay, Phys. Rev. D **32**.695 (1985).
15. W.Pfeil *et. al.*. Electromagnetic properties of hyperons in a relativised quark model, Phys. Lett. B 258 (1991).
16. E.J.Moniz E.Kaxiras and M.Soyeur. Hyperon radiative decay, Phys. Rev. D **32**, 695 (1985).
17. S. Dobbs *et al.*, First measurements of timelike form factors of the hyperons, Λ^0, Σ^0, Σ^+, Ξ^0, Ξ^-, and Ω^-, and evidence of diquark correlations, Phys. Lett. B **739**, 90 (2014).
18. G. Agakishiev *et al.* (HADES Collaboration) Deep Subthreshold Ξ^- Production in Ar+KCl Reactions at 1.76 AGeV, PRL **103**(13) 132301 (2009).
19. G. Agakishiev *et al.* [HADES Collaboration], Eur. Phys. J. A **47** (2011) 21.
20. N.K. Glendenning, Neutron stars are giant hypernuclei ?, APJ **293**, (1985) 470.
21. M. Kotulla *et al.* Technical Progress Report for: PANDA. Strong Interaction Studies with Antiproton. (2005): 1-383.
22. C.Pauly *et al.* Upgrade of the HADES RICH photon detector with H12700 MAPMTs. Nucl. Instrum. Methods. A **876**, (2017).
23. O. Petukhov *et al.* Cosmic tests of Cherenkov Electromagnetic Calorimeter for the HADES experiment, Nucl. Instrum. Methods. A **952**, (2020) 164-167.
24. J. Adamczewski-Musch, *et al*. Production and electromagnetic decay of hyperons: a feasibility study with HADES as a phase-0 experiment at FAIR. Eur. Phys. J. A, **21**, (2021) no 4, p. 1-21.

25. Erni, W. *et al.*, Technical design report for the PANDA (AntiProton Annihilations at Darmstadt) Straw Tube Tracker Eur. Phys. J. A, **49** (2013) no 2.
26. PANDA Collaboration, TDR for the PANDA Forward Tracker (2018).
27. J. Smyrski *et al.*, Pressure stabilized straw tube modules for the PANDA Forward Tracker, J. Instrum. 13, P06009 (2018).
28. D. Przyborowski, *et al.* Development of a dedicated front-end electronics for straw tube trackers in the PANDA experiment. JINST, **11** (2016) no.08, P08009.
29. C. Finck, *et al.*, Nucl. Instrum. Methods. A **508.63** (2003): 63-69.
30. D. Belver *et al.*, "The HADES RPC inner tof wall." Nucl. Instrum. Methods. Phys. Res. A **602.3** (2009): 687-690.
31. A. Zinchenko, *et al.*, A vector-finding approach to track reconstruction in cbm much. CBM Progress Report 2014, edited by V. Friese, and C. Sturm, (GSI, Darmstadt, 2015), 116.
32. S. Jowzaee *et al.*, High-precision measurement of the associated strangeness production in proton-proton interactions Eur. Phys. J. A **52**, 7 (2016) 337.
33. I. Froehlich, *et al.*, PoS ACAT2007, 076 (2007).
34. D. Belver *et al.*, The HADES RPC inner TOF wall. Nucl. Instrum. Methods. A **602**, 687 (2009)
35. J. Adamczewski-Musch *et al.* (HADES), Inclusive Λ production in proton-proton collisions at 3.5 GeV, Phys. Rev. C **95**, 015207 (2017).
36. M. Abdel-Bary *et al.* (COSY-TOF), Production of Λ and Σ^0 hyperons in proton-proton collisions ,Eur. Phys. J. A **46**, 27 (2010).
37. J. Adamczewski-Musch *et al.* (HADES), Inclusive Λ production in proton-proton collisions at 3.5 GeV, Phys. Rev. C **95**, 015207 (2017).
38. G. Hohler, Landolt - Bornstein - Group I Elementary Particles, Nuclei and Atoms. (1983) pp. 7-8.
39. J. Adamczewski-Musch *et al.* (HADES), Σ^0 production in proton nucleus collisions near threshold, Phys. Lett. B **781**, 735 (2018).
40. G. Agakishiev *et al.* (HADES), Baryonic resonances close to the $\bar{K}N$ threshold: The case of $\Lambda(1405)$ in pp collisions, Phys. Rev. C **87**, 025201 (2013).
41. I. Zychor et al. (ANKE), Lineshape of the $\Lambda(1405)$ hyperon measured through its $\Sigma^0\pi^0$ decay, Phys. Lett. B **660**, 167 (2008).
42. S. Taylor **et al.**, Radiative decays of the $\Sigma^0(1385)$ and $\Lambda(1520)$ hyperons, Phys. Rev. C **71**, 054609 (2005).
43. A. Paszke *et al.*, Automatic differentiation in Py-Torch NIPS 2017 Workshop Autodiff (2017).
44. G. Agakishiev *et al.* (HADES), The high-acceptance dielectron spectrometer HADES, Eur. Phys. J. A **41**, 243 (2009).
45. Johannes Siebenson, *et al.* Measurement of the Lambda (1405) in proton proton reactions with HADES, (2010).
46. HADES Collaboration, Proposals for experiments at SIS18 during FAIR Phase-0. No. GSI-2019-00976. Collaboration GSI: HADES, 2017.